

## Measurements of Protons Behind a Polyethylene Shield at NSRL

A. Rusek

April 2009

Collider Accelerator Department  
**Brookhaven National Laboratory**

**U.S. Department of Energy**

USDOE Office of Science (SC), Nuclear Physics (NP) (SC-26)

Notice: This technical note has been authored by employees of Brookhaven Science Associates, LLC under Contract No. DE-AC02-98CH10886 with the U.S. Department of Energy. The publisher by accepting the technical note for publication acknowledges that the United States Government retains a non-exclusive, paid-up, irrevocable, world-wide license to publish or reproduce the published form of this technical note, or allow others to do so, for United States Government purposes.

## **DISCLAIMER**

This report was prepared as an account of work sponsored by an agency of the United States Government. Neither the United States Government nor any agency thereof, nor any of their employees, nor any of their contractors, subcontractors, or their employees, makes any warranty, express or implied, or assumes any legal liability or responsibility for the accuracy, completeness, or any third party's use or the results of such use of any information, apparatus, product, or process disclosed, or represents that its use would not infringe privately owned rights. Reference herein to any specific commercial product, process, or service by trade name, trademark, manufacturer, or otherwise, does not necessarily constitute or imply its endorsement, recommendation, or favoring by the United States Government or any agency thereof or its contractors or subcontractors. The views and opinions of authors expressed herein do not necessarily state or reflect those of the United States Government or any agency thereof.

# Measurements of Protons Behind a Polyethylene Shield at NSRL

Spring 2009

Adam Rusek

## Measurements with Protons at NSRL

While thinking about delivering Solar Particle Event (SPE)-simulation protons onto targets at NSRL, we noted that low energy protons (below 200 MeV), which dominate any SPE spectrum, would undergo severe multiple scattering while drifting through the target room which, therefore, makes delivering a uniformly distributed beam to the end of the room very difficult, if not impossible. The idea was pitched, to use a 20 cm polyethylene degrader just upstream of the target, so that the beam can be delivered at higher energy, thus maintaining its shape in transport, yet be delivered after degrading at a lower energy. If the target is close enough to the degrader, then the beam shape would not deteriorate too much. The questions we then asked were:

1. How bad is the energy straggling introduced by the degrader?
2. How much does the beam shape change with distance from the degrader?
3. How does the dose vary with distance from the degrader? This question is related to scattering and secondary particle production in the degrader.

To try to answer these questions, we made a series of simple measurements with proton beams at various energies. We used several of the 4 hour slots that NSRL Dosimetry received during the NSRL-09A run, spring of 2009.

## Energy Straggling

To get at the energy straggling, we used a combination of thin and thick scintillator system ( $dE/dX$ ,  $\Delta E$ ), shown schematically in figure 1 below. The 200 MeV proton beam was degraded through a 20 cm polyethylene degrader from which it emerged at about 80 MeV and brought to a full stop in the thick scintillator, the output therefore being proportional to the proton's kinetic energy and which is here referred to as the "calorimeter". The thin scintillator is 2 mm thick, which for all but the lowest energy measurements (10-20 MeV KE) can be considered a thin absorber, is referred to as "trigger", the output of which is taken to be proportional to the lineal energy transfer (LET), or  $dE/dX$ .

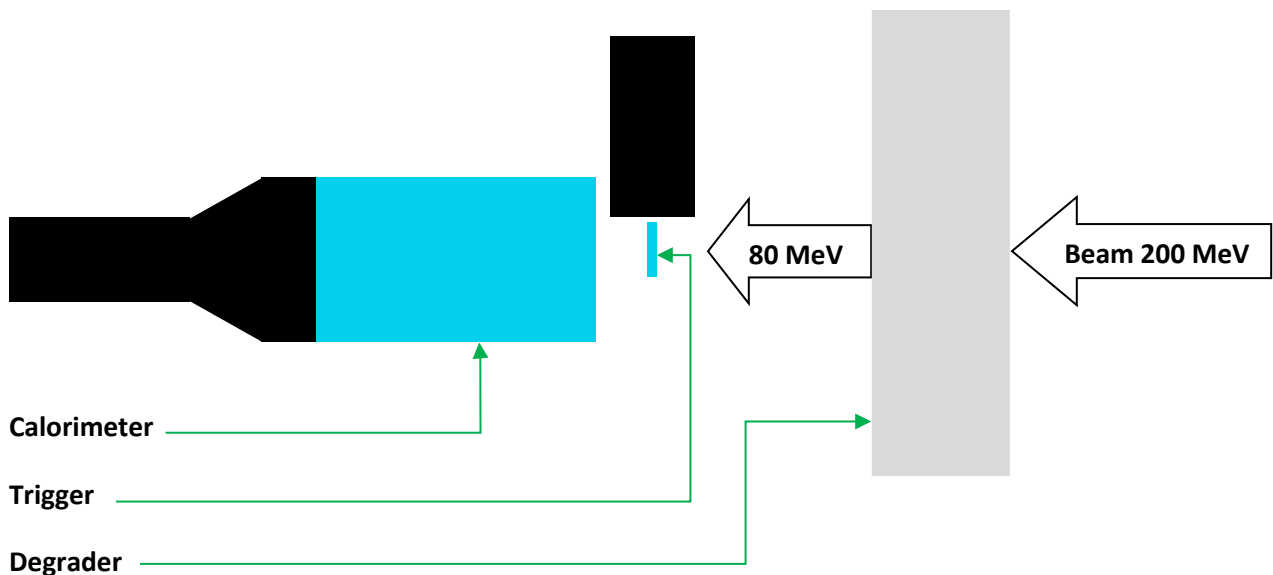


Figure 1

## Calorimetry Data

The pulse heights of the calorimeter and trigger were digitized, event by event, and the values written to data files. The plots of the ADC values are plotted against each other in figure 2 below, with the trigger values along the vertical axis and the calorimeter values along the horizontal one. Five regions are marked on the plot, the events in which are interpreted as follows:

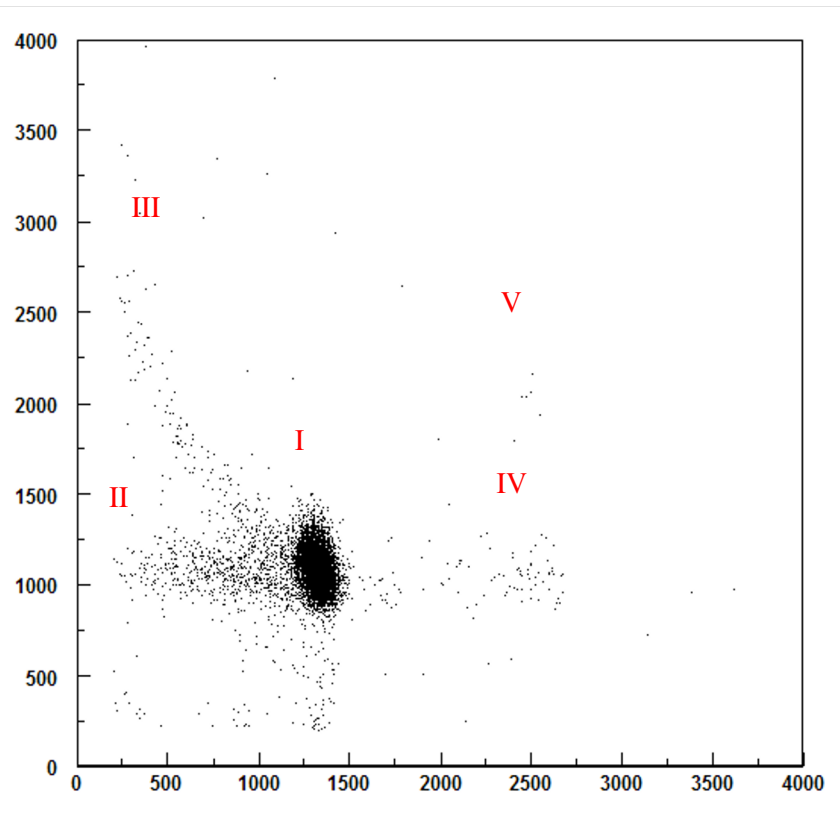


Figure 2

Trigger ADC channels plotted against the calorimeter ADC channels.

### *Region I*

Single protons, at about 80 MeV, which went through the trigger and stopped in the calorimeter, depositing all their remaining energy in it. This group represents about 90.8% of all events.

### *Region II*

Single protons, at about 80 MeV, which went through the trigger, but ended up depositing less energy in the calorimeter, following a nuclear collision in the trigger resulting in either a loss of energy to a knocked-out nucleon, or a large scattering angle such that the proton leaves the calorimeter before coming to a full stop. This group contains 6.1% of all events.

### *Region III*

Single protons, at less than 80 MeV, which went through the trigger and stopped in the calorimeter, depositing all their remaining energy in it. About 2.4% of all events fall into this type.

### *Region IV*

Single protons, at 80 MeV, which went through the trigger, accompanied by a second 80 MeV proton which missed the trigger, but like the first one comes to a full stop in the calorimeter. The pulse height in the trigger corresponds with one proton while that of the calorimeter corresponds with two. About 0.6% of all events fall into this group.

### *Region V*

Two 80 MeV protons that went through both the trigger and the calorimeter. About 0.06% of the events fall into this group.

Of these five regions, only region III is a “contaminant” produced in the degrader. It consists of those protons which emerge from the degrader at lower than the degraded primary energy and amounts to less than 3% of the total tracks.

Next, we reduced the beam energy further by means of the computer-controlled variable-thickness degrader (the binary filter), such that the energies at the exit of the fixed degrader were 10, 20, 30 and 40 MeV.

Figure 3 features five plots, one for each of the energies 10, 20, 30, 40 and 80 MeV. In each plot the trigger counter is plotted along the vertical and the calorimeter along the horizontal axis. The projection on the horizontal, that is, the calorimeter ADC spectrum for each energy, was fitted with a Gaussian, the width measured and recorded, as shown in figure 4. The upper plot is a plot of the five fits, all plotted with the same amplitude. The width of the fit is plotted against the secondary beam energy in the second plot. A likely lowest energy at NSRL is 50 MeV, below which the range is too small to make it of interest to space travel related studies. A beam produced by degrading from 200 to 50 MeV would be spread-out by about 10 MeV (fwhm).

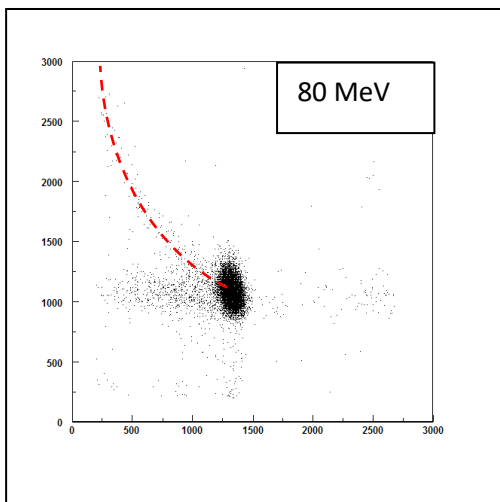
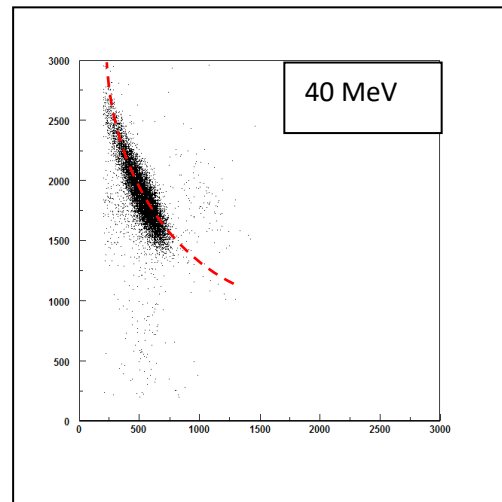
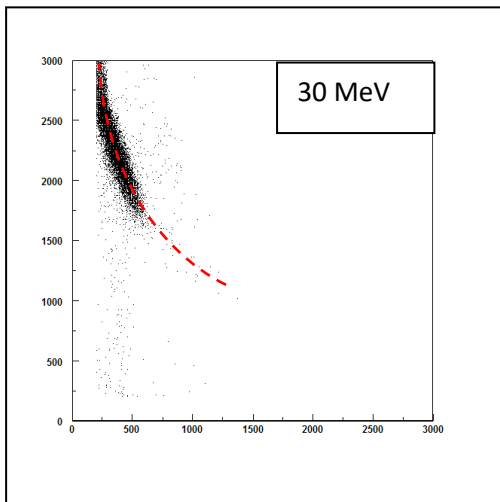
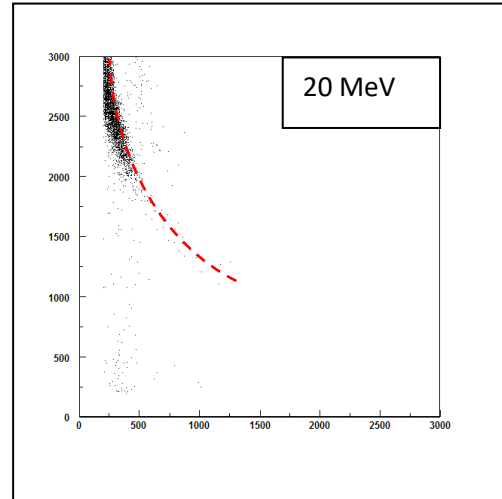
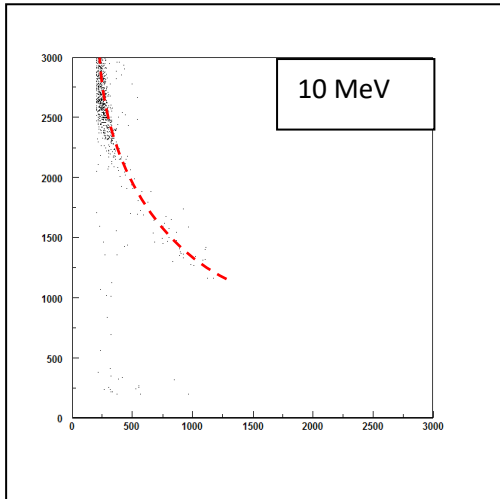


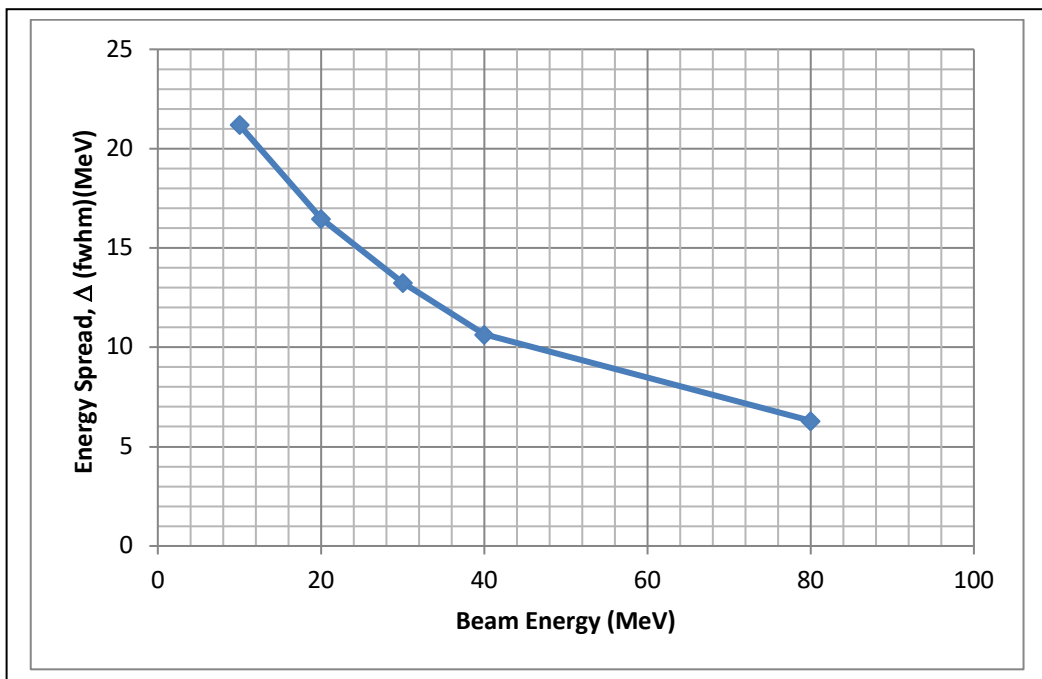
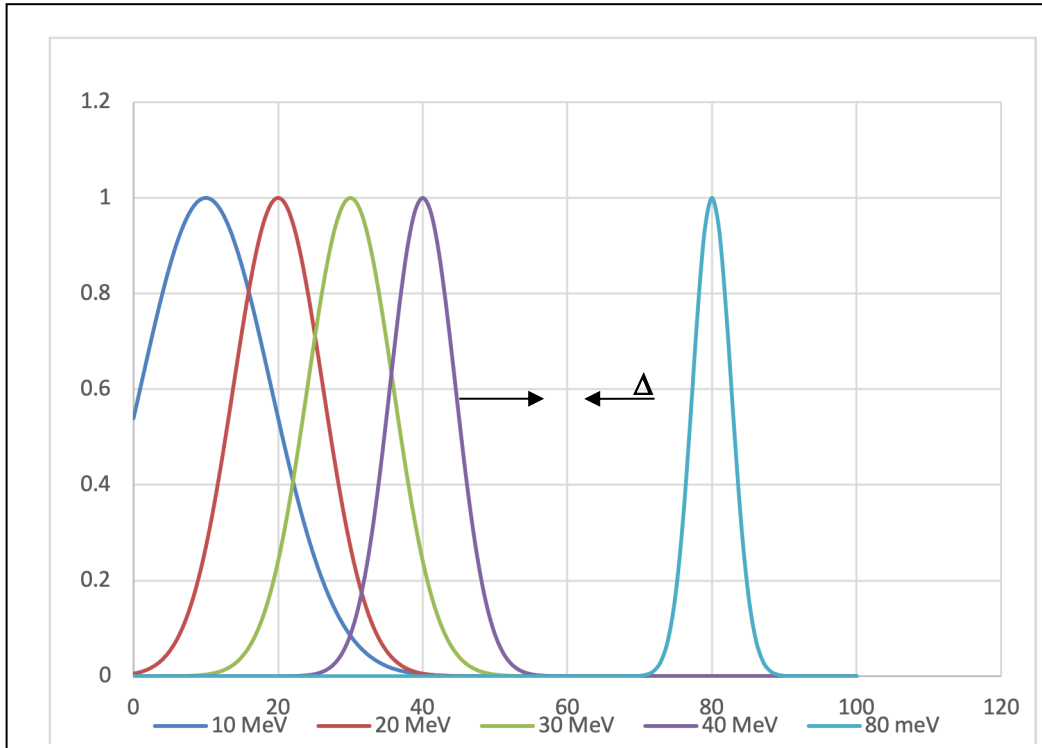
Figure 3:

Event distribution on the LET vs. E plots, for varying energies. The primary beam energy was 200 MeV which, after going through a variable thickness degrader, was reduced to the energies shown on each plot. The axes are in ADC channel number.

Using the peak position in both LET and E for the average value and fitting with a straight line, the conversions from channel number to physical quantities was obtained and is shown below. Goodness of fit in both cases was essentially 1.

$$LET = 0.001973(\text{channel}\# - 116) \text{ MeV}$$

$$E = (0.0564(\text{channel}\# - 130) + 10.663) \text{ MeV}$$



The portion of the spread originating from straggling was determined to be between 93.9% and 99.6%, the number decreasing with increasing energy, as shown in figure 6 below. The portion of the spread



not due to straggling comes from the energy bite at extraction ( $\sim 1\text{MeV}$ ) and the calorimeter resolution ( $< \frac{0.0017}{\sqrt{E}}$ ,  $E$  given in GeV).

The calorimeter resolution was measured using 200 MeV data, for which the spread is dominated by calorimetry resolution (there is no straggling since no degrading is used). The width of the calorimeter distribution was 0.777 MeV ( $\sigma$ ). We assume the form

$$\frac{\sigma}{E} = \frac{C}{\sqrt{E}}$$

and solve for C, given the energy, 200 MeV, at which that data was taken. In the right hand side of the equation the units are GeV:

$$\frac{0.777}{200} = \frac{C}{\sqrt{0.2}}$$

$$C = \frac{0.777(0.4472)}{200} = 0.001737$$

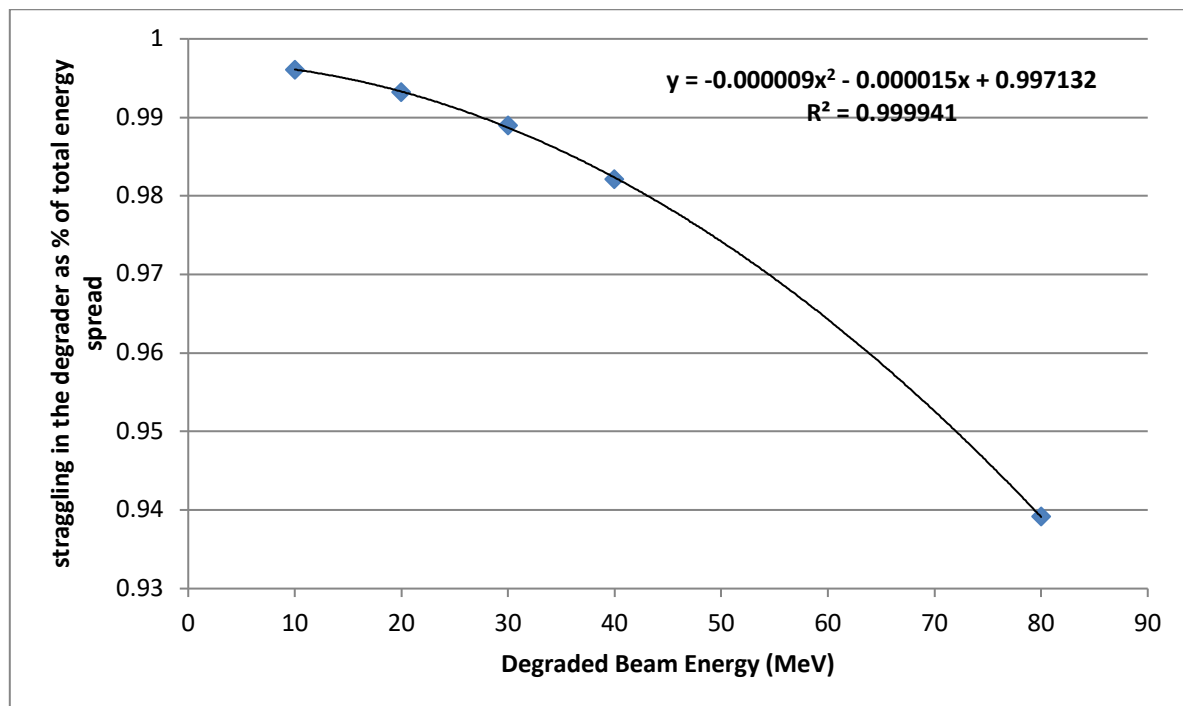
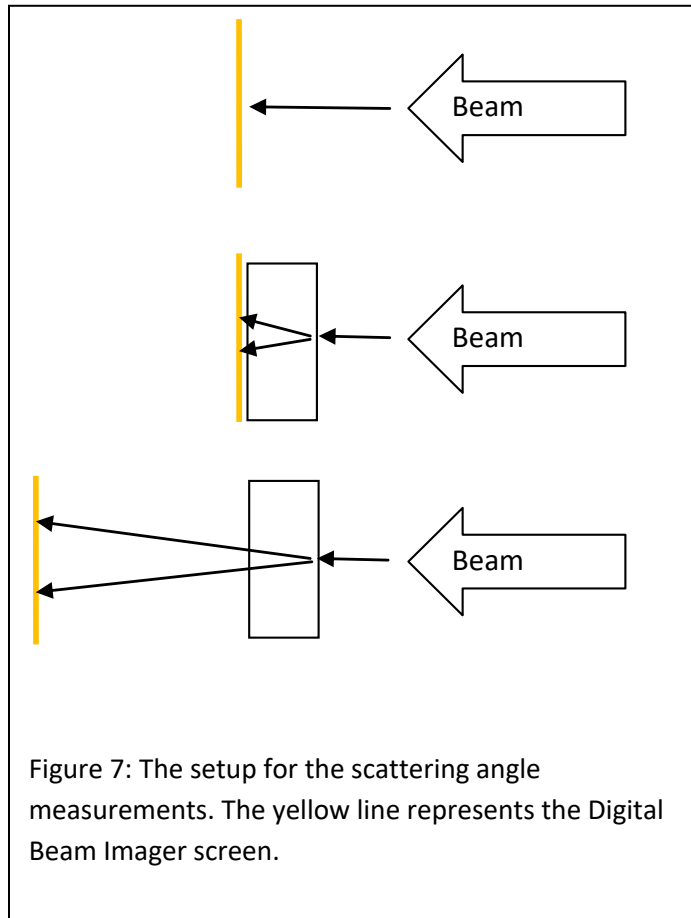


Figure 6: the blue squares are the calculated values. The fit to the points can be used to Predict the straggling at unmeasured points.

## Spread Angle

To measure the spread in the beam introduced by the 20 cm polyethylene degrader we took images of the beam with and without the degrader in place. In the former case, we used two positions for the camera, 0" and 12" from the downstream face of the degrader, as shown in the figure below.



The proton scattering angle after traversing 20 cm of HDP.

1000 MeV: 0.89°

500 MeV: 1.12°

250 MeV: 2.50°

200 MeV: 3.37°

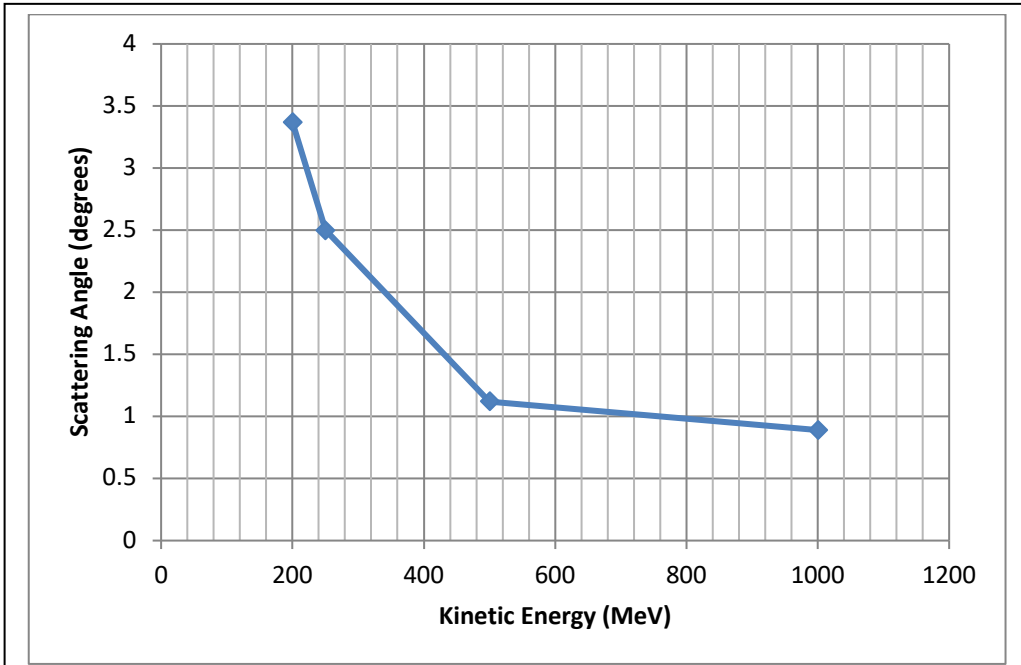
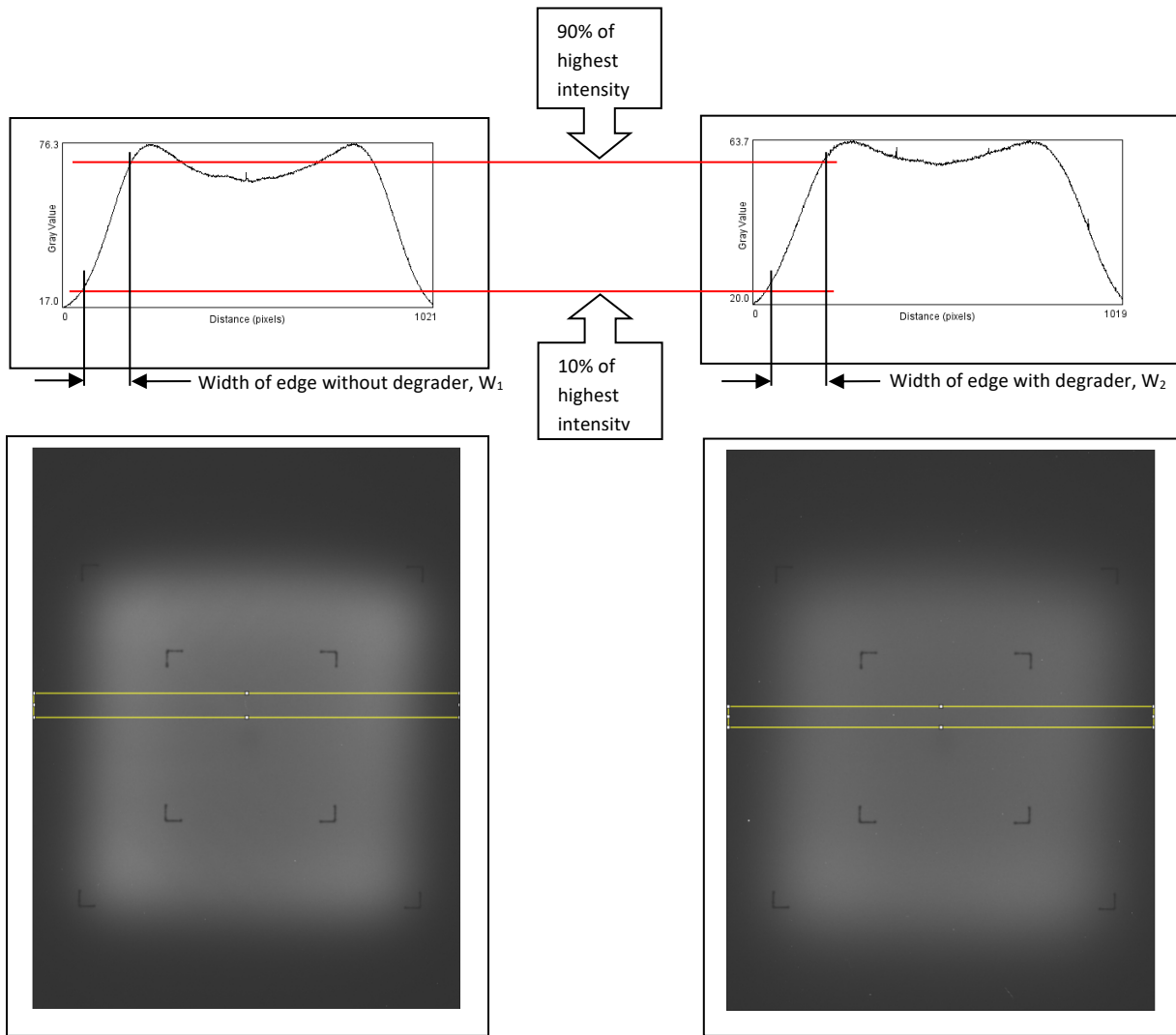


Figure 8: The scattering angle due to 20 cm of polyethylene in beams of various energies.



$$\text{Spread Angle} = \tan^{-1} \left[ \frac{\Delta \text{width}}{D} \right] = \tan^{-1} \left[ \frac{W_2 - W_1}{12''} \right]$$

The technique used to quantify the amount of spreading introduced by a degrader.

## Dose behind a Degradator

For this measurement we placed the degrader in the beam after calibration, and used the calibration chamber to measure the dose downstream from the degrader from 0 to 100 cm away. This was done at 1000, 500, 250 and 200 MeV, and the results of this measurement are shown in figure 9 for the 1000 and 200 MeV cases. The horizontal axis is in cm as measured from the downstream face of the 20 cm polyethylene degrader, and the vertical one is in dose as a percent of the dose incident on the upstream side of the degrader.

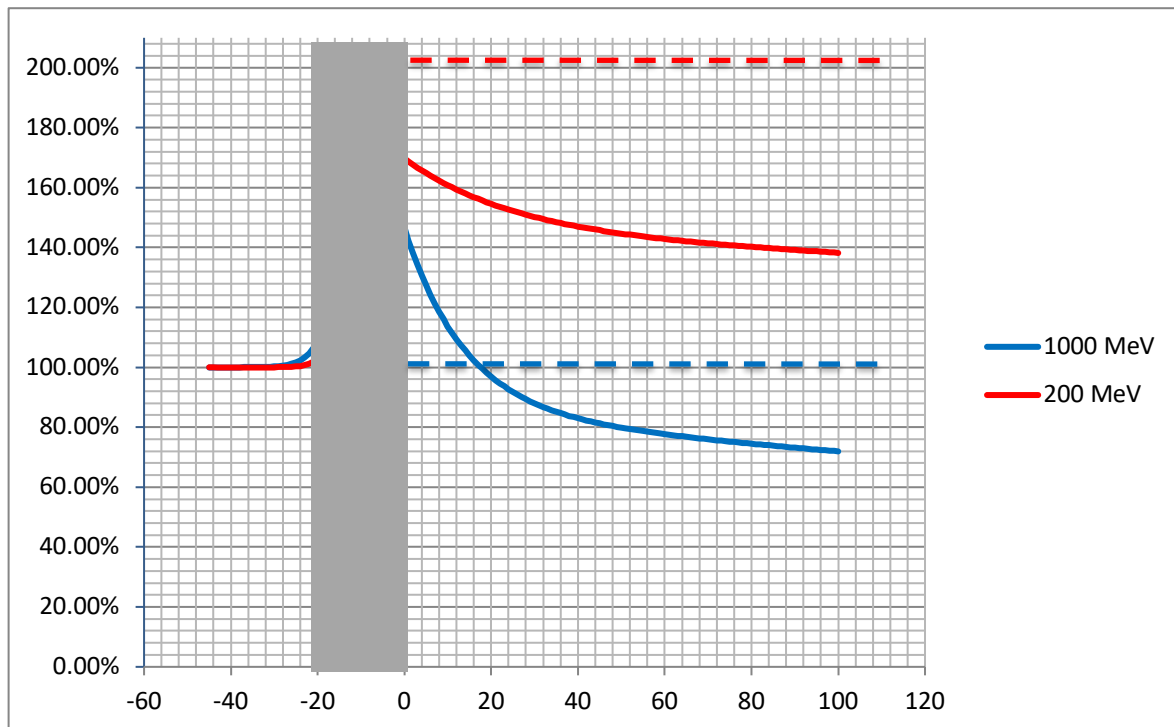


Figure 9

The dashed lines indicate the dose that would be expected if the incident beam was only shifted in energy, and no other effect took place. The reason the actual dose at 100 cm from the degrader is lower is because not all the beam makes it out of the degrader, and that part which does is no longer parallel (see the section on angle spread). The high dose near the degrader is due to the large number of secondary protons produced in the degrader, some at low energy and large scattering angle. This component is largely suppressed as we move away from the degrader, and can be modeled with a model in which it is described as a portion of the beam which has a source some distance upstream of the degrader, and scattering through an angle  $\theta$ .

$$Dose = D_{\infty} + \frac{1}{\pi(R+L)^2 \tan^2 \theta}$$
, where R is the distance from the downstream end of the degrader, L

is the distance from the source to the downstream end of the degrader and  $D_{\infty}$  is the dose at a far enough point, normalized to the incident dose.

Energy	$D_{\infty}$	L (cm)	$\theta$ (deg)
1000 MeV	0.68	30	1.19
200 MeV	1.33	64	0.83